

## Time-lapse FWI using simultaneous sources

He. Liu, Xin. Fu, Daniel. Trad, Kristopher. Innanen  
University of Calgary

### Summary

Full-waveform inversion (FWI) has been used to estimate high-resolution subsurface velocity models. It has become a powerful tool for time-lapse seismic inversion, which is promising to monitor reservoir profile changes with injection and production, and potentially long-term storage of CO<sub>2</sub>. To overcome the challenge of expensive computational costs for FWI process, shot subsampling methods and source-encoding strategies have been used to make the full waveform inversion efficient while maintaining the quality of the inversion results with minimum sacrifice. In this work, we incorporate amplitude-encoding strategy with cyclic subsampled data scheme, which first subsamples the data cyclically and then compose blended during the iterations. In this way, we can directly eliminate much more crosstalk terms introduced by encoded individual shot gathers and reduce the data dimension to improve FWI efficiency. We have applied this strategy to acoustic time-lapse FWI in time domain, and the synthetic inversion results recovered the velocity profile changes in the time-lapse model very well with reduced computation efforts.

### Theory

The simplest subsampling method is regular subsampling, which statically subsamples every  $n$ th specific shot shown in Figure 1a. Since some of the information in the observed data is lost, this scheme degrades the inversion result. To better take the advantage of data information, cyclic subsampling (Ha and Shin, 2013) has been proposed. This method uses every shot the same number of times or at least a similar number of times (Figure 1b). To avoid distance variability between the selected shots, the selected shots in each subgroup are uniformly spaced.

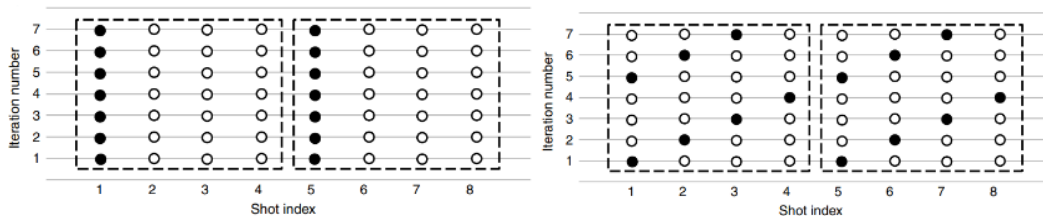


Figure 1. The regular and cyclic subsampling schemes. The black dots indicate the shots used in an iteration (adopted from Ha and Shin, 2013).

An amplitude-encoding method composes individual shot gathers into super shot gathers by the encoding matrix (Godwin and Sava, 2013), which is defined as

$$\mathbf{B} = \begin{bmatrix} b^{1,1} & \dots & b^{N_{sig},1} \\ \vdots & \ddots & \vdots \\ b^{1,N_{sup}} & \dots & b^{N_{sig},N_{sup}} \end{bmatrix}_{N_{sup} \times N_{sig}}$$

where  $N_{sup}$  is the number of the super-shots and  $N_{sig}$  is the number of the individual shots ( $N_{sup} < N_{sig}$ ). The  $N_{sig}$  synthetic data and observed data are blended into  $N_{sup}$  blended data by

$$\mathbf{p}^{sup} = \mathbf{B}\mathbf{p}$$

The ratio between  $N_{sig}$  and  $N_{sup}$  is the factor by which the computational cost is reduced. Since usually  $N_{sup}$  is much smaller than  $N_{sig}$ , the encoding FWI would achieve much better efficiency due to the reduction of data dimension.

## Results

In this section, we use a down-sampled acoustic Marmousi model to test the scheme. The true baseline model is shown in Figure 2a. Two reservoirs are located left and right at mid-depth in the model, respectively. To mimic a fluid change, 150 m/s acoustic velocity changes are added at the two reservoirs as displayed in Figure 2b to obtain the monitor model. A smoothed initial model is displayed in Figure 2c, which is used in FWI of both baseline and monitor models.

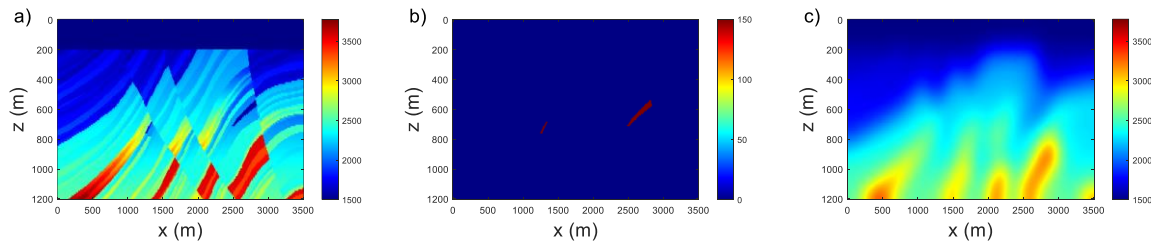


Figure 2: a) True baseline model. b) True time-lapse model. c) The starting model is obtained by smoothing the true baseline model.

The models have a distance of 3500 m and a depth of 1200 m and are discretized by 350 by 120 cells with 10 meters grid spacing. On the top of the model, 174 sources are evenly distributed at the depth of 20 m and 350 receivers are located at each grid point. The source wavelets used for baseline and monitor data sets are identical with a dominant frequency of 10 Hz. The time sampling interval is 1.5 ms and the maximum recording time is 2 s.

We subsample 58 shot gathers to compose 10 super-shots with even spatial distance from all 174 shots and re-subsample the data cyclically every few iterations. Using an amplitude-encoding strategy for all the individual shots, we can get the encoding and crosstalk matrices as shown in Figures 3a and 3c. From the crosstalk matrix, we can notice many non-zero elements off the main diagonal, which represent the coefficients of the crosstalk terms. After applying the cyclic subsampling scheme, we use 58 shots of all the observed data at each iteration to compose super-shots. In Figures 3b and 3d we see the encoding and crosstalk matrices at the first iteration. From the crosstalk matrix, we can notice that compared with Figure 3c, many off-diagonal elements are reduced to zero.

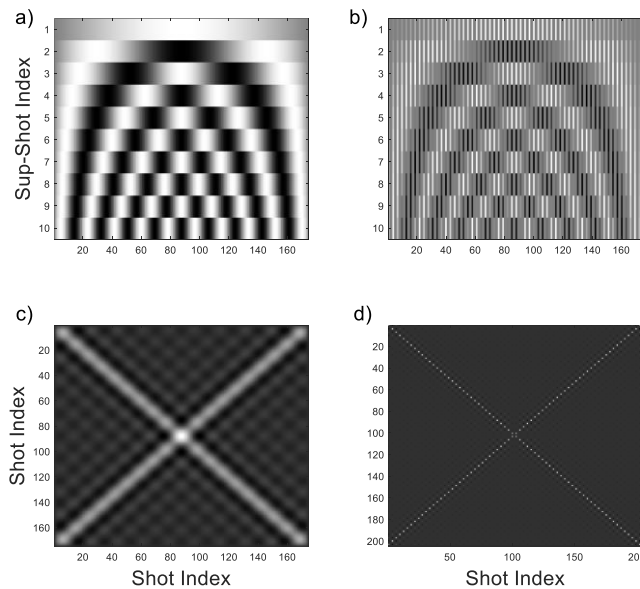


Figure 3: The encoding (first row) and crosstalk (second row) matrices: using all the individual shots (left column) and subsampled shots (right column).

To show the capacity of the time-domain constant-density acoustic FWI program (Yang et al., 2014) used in this study, we first present the inverted baseline model in Figure 4a, and two vertical profiles through the two reservoirs at distances of 1300 m and 2700 m, which are extracted and plotted in Figure 4b. From the final image after 100 iterations shown in Figure 4a, we can see the fine subsurface structures in the Marmousi model are well recovered with no significant crosstalk noise introduced. In Figure 4b, we compare the inverted and true velocity profiles. In this Figure, the solid black lines are the true models, the dashed red lines are starting models, and the yellow lines are inverted baseline models. The reservoirs are located at 740 m and 600 m deep. From the comparison, we can see the black and yellow lines match very well, even though the fine structures at large depths need further updates.

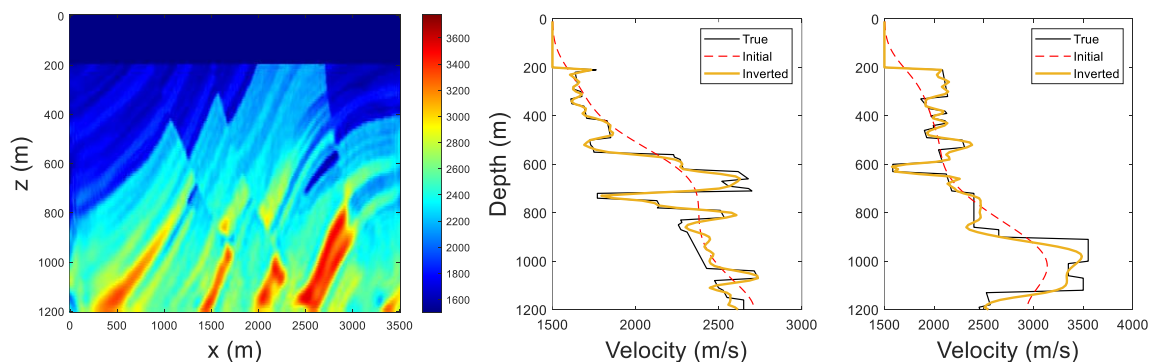


Figure 4. a) Inverted baseline model; b) The solid black lines are the true model, the dashed red lines are starting models, and the yellow lines are inverted baseline models at distance 1300 m (left) and 2700 m (right).

From the inverted baseline and monitor models, we see the technique does not introduce obvious crosstalk noises in the final images. Using a parallel time-lapse FWI strategy, we use the same scheme to invert the monitor model, which is shown in Figure 5b. We show the inverted time-lapse model after subtraction in Figure 5c. We can see the well-inverted velocity changes in the two reservoirs.

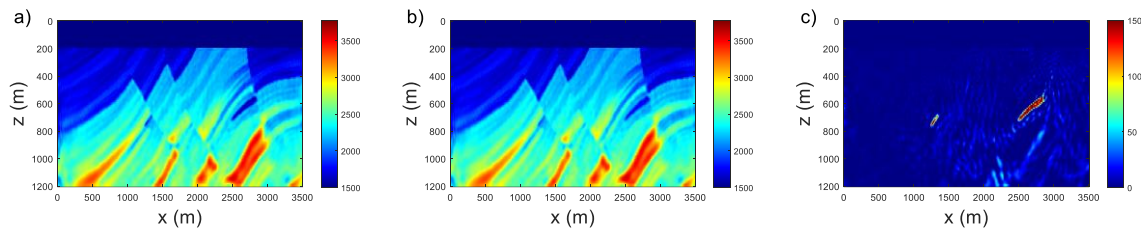


Figure 5: Inverted baseline, monitor and time-lapse models.

## Conclusions

We presented cyclic subsampled data-based amplitude-encoding time-lapse FWI in the time domain. Based on subsampled shots, the number of crosstalk terms in the crosstalk matrix can be significantly reduced. FWI examples show that this combined scheme can make the inversion process efficient with minimum sacrifices in the inversion results.

## Acknowledgements

We thank the sponsors of CREWES for their continued support. This work was funded by CREWES industrial sponsors and NSERC (Natural Science and Engineering Research Council of Canada) through the grant CRDPJ 543578-19. We would also like to thank Dr. Pengliang Yang for his contribution to the acoustic FWI program.

## References

- Godwin, J., and Sava, P., 2013, A comparison of shot-encoding schemes for wave-equation migration: *Geophysical Prospecting*, 61, 391–408.
- Ha, W., and Shin, C., 2013, Efficient Laplace-domain full waveform inversion using a cyclic shot subsampling method: *Geophysics*, 78(2), R37-R46.
- Yang, P., Gao, J., and Wang, B., 2015, A graphics processing unit implementation of time-domain full waveform inversion: *Geophysics*, 80, No. 3, F31–F39.